Charge confinement in heterojunction acoustic charge transport devices

G. A. Peterson, B. J. McCartin, W. J. Tanski, and R. E. LaBarre

Citation: Applied Physics Letters **55**, 1330 (1989); doi: 10.1063/1.101646
View online: http://dx.doi.org/10.1063/1.101646
View Table of Contents: http://scitation.aip.org/content/aip/journal/apl/55/13?ver=pdfcov
Published by the AIP Publishing

Charge confinement in heterojunction acoustic charge transport devices

G. A. Peterson, B. J. McCartin, W. J. Tanski, and R. E. LaBarre
United Technologies Research Center, East Hartford, Connecticut 06108

(Received 25 April 1989; accepted for publication 18 July 1989)

An equilibrium model is developed for charge confinement in heterojunction acoustic charge transport (HACT) devices. The Poisson–Boltzmann equation is solved for the self-consistent potential and packet charge distribution in a surface acoustic wave (SAW) superimposed on a (Al,Ga)As/GaAs heterostructure. Numerical results are presented for the charge capacity of a 275 MHz HACT configuration. For a 1 V SAW potential, the charge capacity is limited by the heterojunction well depth rather than by space-charge lowering of the SAW barrier.

Acoustic charge transport devices are promising for wide-bandwidth (up to 500 MHz) analog signal processors and rf memories. In these devices injected signal charge is longitudinally confined and transported by the piezoelectric potential generated in a propagating surface acoustic wave (SAW). At present there are two varieties of such devices differing in the mode of transverse (i.e., vertical) charge confinement: (i) HACT[1] (heterostructure acoustic charge transport) and (ii) its predecessor, ACT.[2] In HACT charge is confined transversely in a potential well formed by two (Al,Ga)As/GaAs heterojunctions, whereas in ACT it is confined by a depletion potential in the epilayer. The depletion potential is generated by a back-biased Schottky barrier and an applied back-gating potential. In each of these technologies, the charge-carrying capacity of the confining wells is a critical issue since device performance, e.g., dynamic range and bandwidth, is limited by the space-charge lowering of the barriers. The purpose of this letter is to report a self-consistent approach for calculating the distribution of charge in a packet and to present results on the charge-carrying capacity of HACT devices.

A prototype HACT configuration is shown in Fig. 1. Since typical well widths are $\sim$400 Å and charge densities are $< 10^{16}/\mathrm{cm}^3$, both the quantum subband intervals and the Fermi energy are much less than either the barrier height or kT, where k is the Boltzmann constant and T the temperature. Under these conditions, a purely classical description suffices. In our model the charge packet is assumed to be in thermal equilibrium in the co-moving (i.e., SAW) frame of reference. With this assumption the mobile charge density $n(x,y)$ follows a Boltzmann distribution:

$$\begin{aligned} n(x,y) &= n_0 e^{q\phi/kT} && \text{(inside the well)}, \\ &= n_0 e^{-\Delta E_c/kT e q\phi/kT} && \text{(outside)}, \end{aligned} \tag{1}$$

where ΔE_c is the heterojunction conduction-band offset, n_0 a parameter set by the packet charge, q the magnitude of the electric charge, and ϕ the electrostatic potential. Ignoring distortions in the charge distribution due to the synchronous field, which are small, the resultant nonlinear Poisson–Boltzmann equation for the charge distribution in a HACT device reads

$$\nabla^2\phi = (4\pi q/\epsilon)(n - n_{\mathrm{SAW}} - n_d), \tag{2}$$

where n_{SAW} and n_d are, respectively, the piezoelectric charge distribution generated by the SAW wave and the net doping profile and ϵ is the dielectric constant. The polarization charge is simply derived from the SAW potential ϕ_{SAW}. [$n_{\mathrm{SAW}} = -(\epsilon/4\pi q)\nabla^2\phi_{\mathrm{SAW}}$]. Various approximate forms for ϕ_{SAW} have been used in this study. This approach differs significantly from that previously reported for ACT which assumes strict charge neutrality in the packet,[3] or, equivalently, a zero Deybe length. More recently, however, Bogus has used a steady-state device model to analyze charge injection in ACT.[4]

The relationship between n_0, which parameterizes the electron density, and N, the charge/cm in the packet, is not known *a priori*. Mathematically, for a fixed N, n_0 is a nonlinear eigenvalue. The solution strategy adopted here is to solve Eq. (1) parametrically in n_0 and to find $\phi(r,n_0)$. Using this, a post processing integration then determines $N(n_0)$, i.e.,

$$N = n_0 \int\int dx\, dy\, e^{q\phi(x,y,n_0)/kT}. \tag{3}$$

A series of increasingly realistic boundary conditions was tried. In the horizontal direction, the solution domain is one SAW wavelength, $\lambda = 10\ \mu$m. Neumann or periodic boundary conditions are imposed at the ends, i.e.,

$$\frac{\partial\phi(x,y)}{\partial x} = 0 \quad \text{at } z = \pm\frac{\lambda}{2}. \tag{4}$$

These periodic solutions represent HACT operation at low signal frequencies for which packet-to-packet variations are

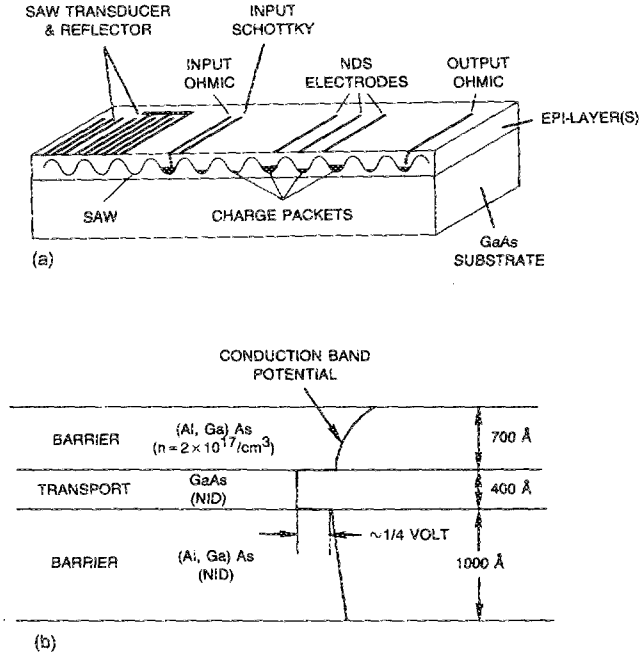

FIG. 1. Schematic illustrations of (a) basic HACT operation and (b) the heterostructure configuration with corresponding band-edge diagram.

 0003-6951/89/391330-03$01.00

on a spatial scale slow compared to a wavelength. At the other extreme, as the signal sampling frequency approaches the Nyquist sampling rate, the solution domain should be enlarged to cover the signal period. Different signal charges in different packets can be accommodated by assigning a separate n_0 for each SAW period. In the vertical direction, the model sets up top and ground planes at large, but finite distances from the HACT surface, i.e.,

$$\phi(x,y) = 0 \quad \text{along } z = \pm d. \tag{5}$$

These ground planes are a necessary artifact of the model, necessary for mathematical closure. In the limit as $d \gg \lambda$, their presence should not influence the solution. Indeed, calculations comparing ground plane separations of 10 μm to those at 20 μm show an approximate 10% variation in computed charge capacity. Finally, the free (Al,Ga)As surface has a high density of occupied surface states. The surface charge density σ is just sufficient to produce a 0.8 eV depletion potential. This leads to a surface charge density of $\sigma \sim 1.4 \times 10^{12}/\text{cm}^2$. These charged surface states are modeled as a discontinuity in the dielectric displacement, i.e.,

$$\left(\frac{\partial\phi(x,y)}{\partial y}\right)_{\text{free}} - \epsilon\left(\frac{\partial\phi(x,y)}{\partial y}\right)_{\text{(Al,Ga)As}} = 4\pi\sigma q. \tag{6}$$

Our device simulation code, NAME II, was successfully applied to the numerical solution of Eq. (2). NAME II is a two-carrier, two-dimensional, steady-state device code which numerically solves the coupled Poisson and transport equations.[5] The code contains a general discretization scheme based on the control area description (or equivalently, the conservation form of the partial differential equations). A unique feature is the use of the Dirichlet regions as the control areas. These in turn are constructed from the Delaunay triangulation of the grid points. This construction naturally resolves the ambiguities arising from negative areas. The nonlinear solver consists of two steps: first, a steepest descent step that gives a global convergence, albeit slow, followed by a Newton iteration that gives fast local convergence. The linear solver is the nonsymmetric, Yale Sparse Matrix package.

Calculations were carried out on a Convex C210 minisupercomputer. For the calculations reported here the SAW profile was assumed to be a plane wave, i.e.,

$$\phi_{\text{SAW}}(x,y) = \phi_0 \cos(kx - \omega t). \tag{7}$$

Insofar as the electrons are confined to the HACT channel, the above approximation suffices and a series of calculations was run parametric in the SAW amplitude ϕ_0.

Numerical results and graphical output were obtained for the self-consistent potential and charge distribution throughout the device. A nominal HACT configuration was chosen as follows (cf. Fig. 1): (1) a 200 Å GaAs cap layer, not intentionally doped (NID); (2) a 700 Å doped $(Al_{0.3},Ga_{0.7})As$ layer ($n_d \sim 2 \times 10^{17}/\text{cm}^3$); (3) a 400 Å GaAs layer transport well (NID); (4) a 1 μm (Al,Ga)As buffer layer; and (5) a thick, nonconducting substrate. For the purposes of these calculations a common dielectric constant $\epsilon = 13$ was taken for all the layers.

A series of computer runs was carried out varying the following parameters: (i) N, the charge/cm per packet or

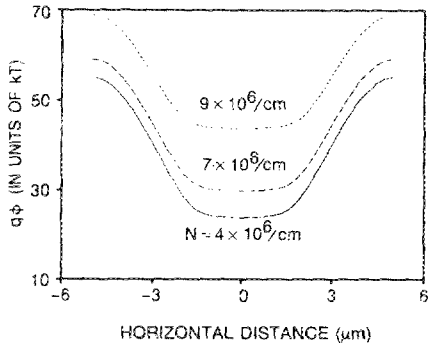

FIG. 2. Horizontal cuts of the self-consistent potential energy surface for charge loads of $N = 4$, 7, and 9×10^6 charges/cm. Note the space-charge lowering of the SAW potential barrier.

more precisely, as discussed above, n_0, the charge distribution parameter, (ii) ϕ_{SAW}, the amplitude of the SAW piezoelectric potential, and (iii) d, the ground plane separation. Results reported herein are specifically for $\phi_{\text{SAW}} \sim 1$ V, a nominal experimental value,[1] and for a ground plane separation of 20 μm. Figure 2 shows horizontal cuts of the self-consistent potential energy surface through the center of the HACT channel for several different values of the injected charge load, N. For small N the potential is nearly that of the bare, piezoelectric SAW potential; but as N increases, this potential is shielded by the injected charge and the confining SAW barrier is lowered. Another effect is that the channel potential energy is raised with respect to both ground and the adjacent epilayer by the space charge confined in the well. This effect is better illustrated in Fig. 3 which shows a vertical cut through the center of the conduction-band-edge surface, again for several different values of N. (Comparing Figs. 2 and 3, the conduction-band edge at the center of the well is just 0.4 eV or 10 kT below the potential energy.)

Eventually, with increasing packet charge, a value N_c is reached above which it is more likely that additional charge will go into the buffer layer than into the GaAs well. This happens when the potential in the buffer layer is within a few kT of the bottom of the well. For the HACT configuration considered here, the calculated value of N_c is 9×10^6 charges/cm. The corresponding calculated integrated charge in the buffer layer is 10^6 charges/cm or approximately 10% of the total. The calculations show that the excess

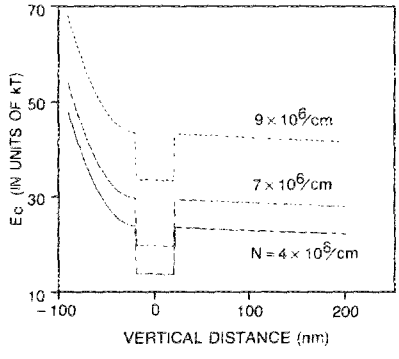

FIG. 3. Vertical cuts of the conduction-band-edge surface through the center of the HACT device for charge loads $N = 4$, 7, and 9×10^6 charges/cm. Note the increasing well energy with increasing packet charge.

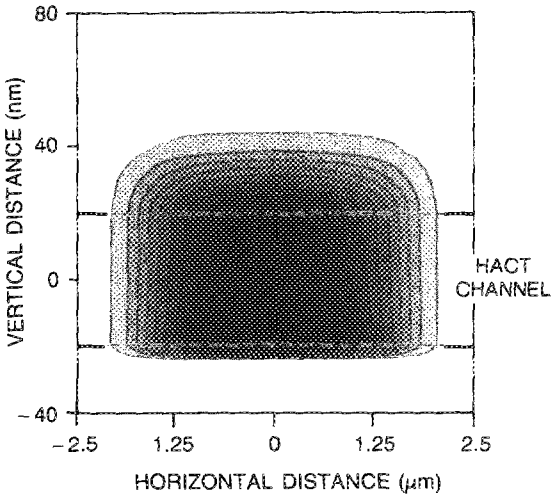

FIG. 4. Charge density contours in the region of the HACT channel for $N = 9\times10^6$ charges/cm. Contour intervals are $\Delta n = 0.8\times10^{15}$ charges/cm^3.

epilayer charge is preferentially located along the buffer layer-substrate interface. (Figure 4 displays the charge contours for $N\sim9\times10^6$ charges/cm within and in the neighborhood of the well. Charge within the well is concentrated on the epilayer side.) It is important to note that for this value of N_c, the effective SAW barrier is ~25 kT which confines the charge in the horizontal direction (cf. Fig. 2).

Taking N_c as a measure of the charge capacity N_{cap}, the present calculated value of 9×10^6 charges/cm is in reasonable agreement with experimental results.[3] Prior measurements of the current at zero input bias give $N_{cap}\sim12\times10^6$ charges/cm. Possible explanations for the difference between the calculated and measured charge capacities are (i) excess charge in the buffer layer is synchronously transported by the SAW, or (ii) the potential is modified by charged interfacial states at the buffer-substrate interface.

In this interpretation, the charge capacity of the HACT device is limited by the repulsive potential generated by the space charge in the channel; i.e., the channel becomes electrostatically less attractive than the epilayer. (There is, of course, no lowering of the heterojunction barrier ΔE_c.) This suggests that the charge capacity can be increased by increasing ΔE_c and, indeed, this has been confirmed by calculations. The situation in ACT devices is somewhat different. There, the SAW barrier lowers continuously and a criterion on the charge transfer efficiency effectively limits the charge capacity (which is much lower than the charge which will buckle the confining potential).

In summary, theoretical methods for self-consistently analyzing the charge confinement have been devised and successfully applied to HACT. The results show that the $(Al_{0.3},Ga_{0.7})As/GaAs$ heterojunction (and not the SAW) barriers limit the charge capacity.

The authors gratefully acknowledge the contributions of K. Dauphinais, D. E. Cullen, S. W. Merritt, and R. H. Sacks.

[1]W. J. Tanski, S. W. Merritt, R. N. Sacks, D. E. Cullen, E. J. Branciforte, R. D. Carroll, and T. C. Eschrich, Appl. Phys. Lett. **52**, 18 (1988).
[2]M. J. Hoskins, H. Morkoc, and B. J. Hunsinger, Appl. Phys. Lett. **41**, 332 (1982).
[3]M. J. Hoskins and B. J. Hunsinger, J. Appl. Phys. **55**, 413 (1984).
[4]E. G. Bogus, Ph.D. thesis, University of Illinois, 1987.
[5]B. J. McCartin, R. H. Hobbs, R. E. LaBarre, and P. E. Kirschner, *Proceedings of the 4th International Conference on Numerical Analysis of Semiconductor Devices and Integrated Circuits* (Boole, Dublin, 1985), p. 411.